doi:10.2533/chimia.2012.675 Chimia 66 (2012) 675–680

Perovskite-supported Palladium for Methane Oxidation – Structure–Activity Relationships

Arnim Eyssler, Ye Lu, Santhosh Kumar Matam, Anke Weidenkaff, and Davide Ferri*

Abstract: Palladium is the precious metal of choice for methane oxidation and perovskite-type oxides offer the possibility to stabilize it as PdO, considered crucial for catalytic activity. Pd can adopt different oxidation and coordination states when associated with perovskite-type oxides. Here, we review our work on the effect of perovskite composition on the oxidation and coordination states of Pd and its influence on catalytic activity for methane oxidation in the case of typical Mn, Fe and Co perovskite-based oxidation catalysts. Especially X-ray absorption near edge structure (XANES) spectroscopy is shown to be crucial to fingerprint the different coordination states of Pd. Pd substitutes Fe and Co in the octahedral sites but without modifying catalytic activity with respect to the Pd-free perovskite. On $LaMnO_3$ palladium is predominantly exposed at the surface thus bestowing catalytic activity for methane oxidation. However, the occupancy of B-cation sites of the perovskite structure by Pd can be exploited to cyclically activate Pd and to protect it from particle growth. This is explicitly demonstrated for $La(Fe,Pd)O_3$, where catalytic activity for methane oxidation is enhanced under oscillating redox conditions at 500 °C, therefore paving the way to the practical application in three-way catalysts for stoichiometric natural gas engines.

Keywords: Automotive catalysis · Octahedral coordination · Methane · Palladium · Perovskite

Introduction

Perovskite-type oxides of general formula $ABO_{3\pm\delta}$, where *A* is typically a lanthanide or alkaline-earth element in twelvefold coordination and *B* a transition metal in sixfold coordination (BO_6 octahedra), are mixed-oxide oxidation catalysts with intriguing properties.[1] Substitution of either the *A*- or *B*-site cation is considered a suitable strategy to tune both the stability to exposure to high temperature and the efficiency for various catalytic reactions. For some practical applications like car exhaust aftertreatment where reductive operation periods are periodically applied, addition of a precious metal by the partial substitution of *B*-site cation[2] or by mixing the perovskite-type oxide with a conventional non-perovskitic formulation[3] results in suitable conversion efficiencies of pollutants. The former situation is the subject of this contribution. The protective function of the perovskite-type oxide towards particle growth of precious and transition metals was already recognized in the early studies.[4] However, the structural redox 'breathing' of a perovskite-type oxide has provided renewed interest for the combination with a precious metal, especially where the precious metal is required for low-temperature activity and for reduction activity. Addition of Pd to $LaFeO_3$ generates a promising three-way catalyst for the exhaust aftertreatment of gasoline engines that was commercialized in Japan.[2] Under the oscillating redox conditions and after exposure to high temperature, $LaFeO_3$ is able to avoid extensive Pd particle growth observed on the conventional catalyst, a major source of efficiency loss of automotive catalysts with mileage. Pd can reversibly enter the perovskite lattice under oxidizing conditions and exsolve under reducing conditions. This strong interaction was also exploited to develop a $PtO_x/LaFeO_3$ catalyst for NO and N_2O reduction.[5]

The scarce global oil reserves together with the increasing number of vehicles worldwide and the progressively severe emission regulations call for alternative fuels and as a consequence for targeted exhaust after-treatment technologies. In this context, the Swiss Federal Laboratories for Materials Science and Technology (Empa) are developing mid-class passenger vehicles based on the use of natural gas (composed of >90% CH_4). The current commercial after-treatment technology for stoichiometric natural gas fuelled engines is based on three-way catalysts (TWC) enriched in Pd, recognized as the major active precious metal for CH_4 oxidation. Beside CO and NO_x pollutants, engine CH_4 emissions need to be treated catalytically because of its larger global warming potential than CO_2.[6] Since perovskite-type oxides are excellent CH_4 oxidation catalysts[7] and are promising TWC of natural gas engines when modified with palladium,[8] we have initiated a research line directed towards the systematic understanding of the structure of precious metal-substituted perovskite-type oxides and its influence on catalytic activity for the specific case of CH_4 oxidation as model reaction. Against the background provided by the work on $LaFe_{0.95}Pd_{0.05}O_{3\pm\delta}$ for gasoline vehicles, we have started to consider the influence of the structure of Pd in the same catalyst formulation but for CH_4 oxidation under steady state and oscillating redox conditions. Since $LaFeO_3$ is not very active for CH_4 oxidation, the major questions are whether the protective function exerted by the perovskite-type structure is a general feature of typical oxidation catalysts (ferrate, cobaltate and manganate) and whether it can be exploited in the case of natural gas operation. In this contribu-

*Correspondence: Dr. D. Ferri
Empa
Swiss Federal Laboratories for Materials Science and Technology
Laboratory for Solid State Chemistry and Catalysis
Ueberlandstrasse 129
CH-8600 Dübendorf
Tel.: +41 58 765 4609
Fax: +41 58 765 1013
E-mail: davide.ferri@empa.ch

tion, we review our results obtained over the past five years.

Where is Palladium?

Determination of the oxidation- and coordination state of palladium in perovskite-type oxides by XRD is difficult because of the fine dispersion of the Pd-containing phase and especially because of the overlap of the perovskite reflexes with those of PdO. The oxidation and coordination states of palladium are better investigated using X-ray absorption near edge structure (XANES) spectroscopy, which is also excellently suited for *in situ* studies. The XANES spectra of two samples are presented in Fig. 1(a). $La(Fe,Pd)O_3$ was prepared by the amorphous citrate method[11] by directly mixing La, Fe and Pd precursors and citric acid, followed by drying on the rotary evaporator and in the vacuum oven at 70 °C and by calcination at 700 °C for 2 h.[9] On the other hand, a second sample designated as $PdO/LaFeO_3$ was prepared by impregnation of $LaFeO_3$ by keeping the Pd loading at 2 wt%. Both spectra indicate that palladium is oxidized. However, the spectrum of $PdO/LaFeO_3$ is very similar to that of dispersed PdO on Al_2O_3. Therefore, Pd in this sample is present on average as Pd^{2+} in square planar coordination as is the case of Pd in PdO particles. This conclusion is strongly supported by XPS.[9] Pd exhibits different oxidation and coordination states in $La(Fe,Pd)O_3$. The high energy edge position of the corresponding XANES spectrum suggests that the oxidation state is higher than in $PdO/LaFeO_3$ and typical supported PdO. XPS results indicate that Pd is in a higher oxidation state than 2+. Additionally, the whiteline of the XANES spectrum is very different from that of PdO and presents a doublet (ΔE = *ca.* 11 eV) that can be taken as the fingerprint of Pd occupying octahedral Fe sites and therefore in octahedral coordination inside the $LaFeO_3$ framework.[9] The following evidence supports this conclusion. The simulated spectrum of $La(Fe,Pd)O_3$, based on full multiple scattering theory[9] clearly shows the doublet observed in the experimental spectrum (Fig. 1(a)). Further, a similar XANES spectrum with the characteristic doublet is observed for $LaPdO_3$. The origin of the peak 11 eV higher than the whiteline was associated by Kim *et al.* to a shake up process involving 1s→5p transitions in the octahedral system,[12] but still deserves deeper investigation. Additionally, the doublet is also observed in the XANES spectra of the self-regenerative catalyst ($LaFe_{0.95}Pd_{0.05}O_{3\pm\delta}$),[13] though the interpretation of the reversible change of structure of Pd in oxidizing and reducing environments was based mainly on the shift of the Pd edge energy. The observation that also other elements in distorted octahedral coordination display a doublet in the whiteline of the XANES spectrum supports our interpretation.[14]

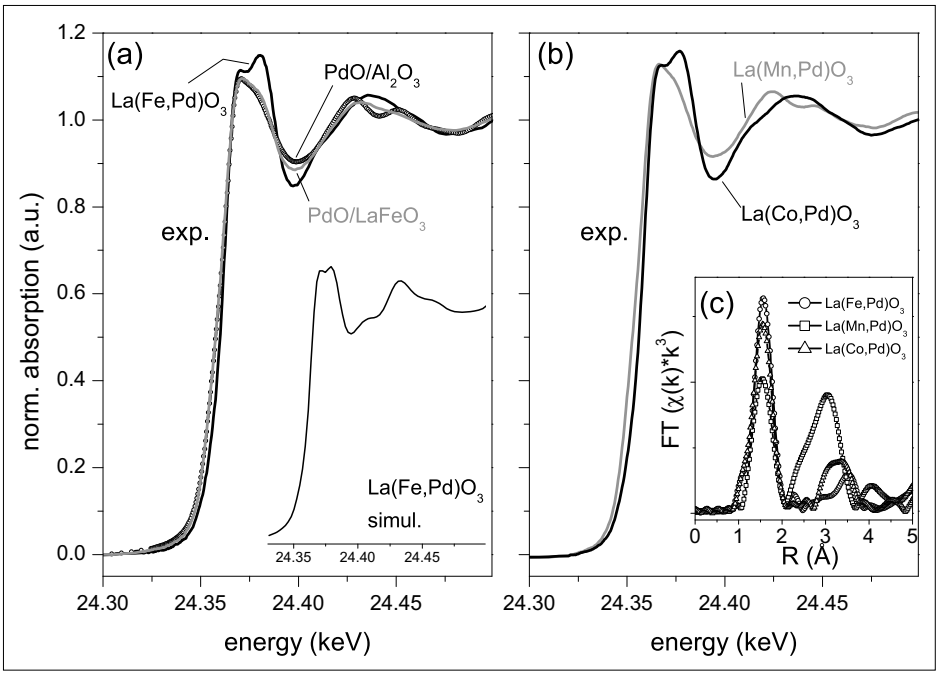

Fig. 1. Transmission XANES spectra at the Pd K-edge of (a) $La(Fe,Pd)O_3$, $PdO/LaFeO_3$, and PdO/Al_2O_3; (b) $La(Mn,Pd)O_3$ and $La(Co,Pd)O_3$. The simulated spectrum of $LaFe_{0.95}Pd_{0.05}O_3$ is also reported in (a) for comparison. (c) Corresponding FT-EXAFS. Adapted from refs. [9] and [10].

The nature of the different Pd species identified using XANES can be further verified by probing their stability under reducing conditions, *i.e.* using hydrogen temperature programmed reduction (H_2-TPR). Under H_2-TPR conditions, $PdO/LaFeO_3$ partly reduces already at room temperature, which is typical of supported Pd nano-particles (Fig. 2). At 300 °C, the spectrum resembles that of metallic Pd supported on conventional oxide supports. In strong contrast, $La(Fe,Pd)O_3$ reduces slowly and at 300 °C the XANES spectrum does not present any evident feature of metallic Pd. Reduction occurs as indicated by the shift of the edge energy to lower values (arrows in Fig. 2). The different reduction behaviour of $La(Fe,Pd)O_3$ is associated with the slow segregation of Pd and

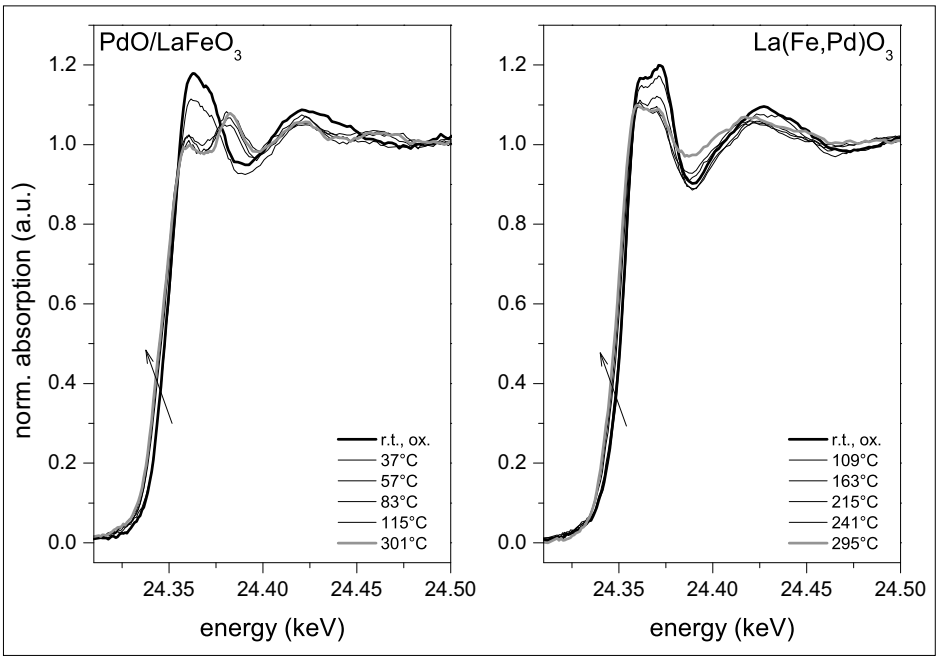

Fig. 2. Selected *in situ* transmission XANES spectra at the Pd K-edge during H_2-TPR of $PdO/LaFeO_3$ and $La(Fe,Pd)O_3$ (5 vol% H_2/He). The arrows indicate the shift of energy upon reduction. Adapted from ref. [9].

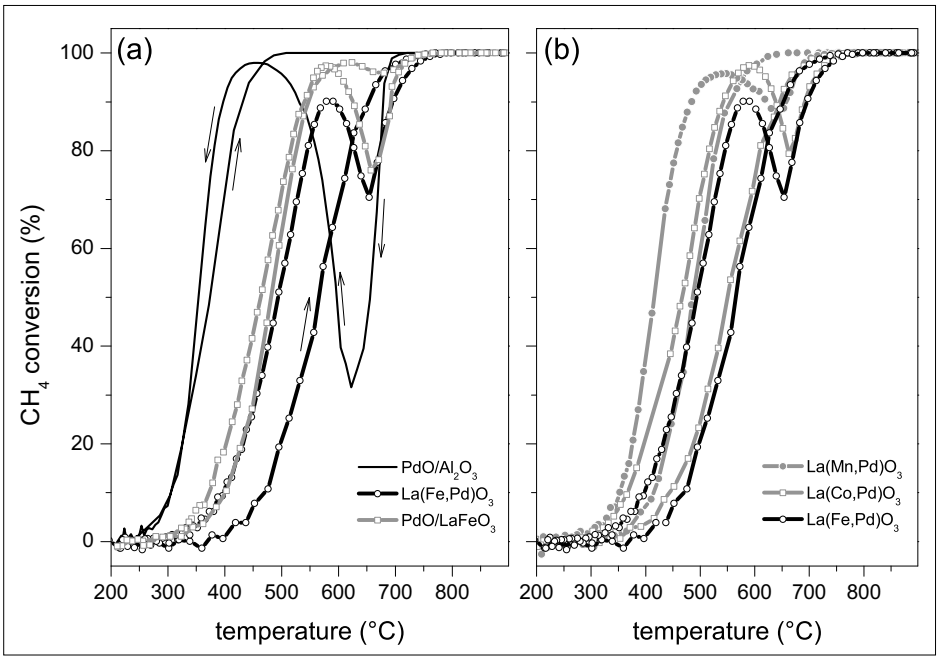

Fig. 3. Methane oxidation activity profiles of (a) $La(Fe,Pd)O_3$, $PdO/LaFeO_3$ and PdO/Al_2O_3, and (b) $La(Mn,Pd)O_3$, $La(Fe,Pd)O_3$ and $La(Co,Pd)O_3$ during a full heating-cooling cycle between 200 °C and 900 °C. Adapted from refs. [9] and [10].

the formation of small Pd domains that do not yet show the typical EXAFS oscillations of structured Pd nano-particles at this temperature. The *in situ* XANES data well reflect conventional H_2-TPR experiments showing a single reduction peak at 86 °C and a broad one at 270 °C for $PdO/LaFeO_3$ and $La(Fe,Pd)O_3$, respectively.[9]

The characterization data show that Pd adopts at least two different oxidation and coordination states in $LaFeO_3$ depending on the different synthesis routes. When the Pd salt is added to the precursor solution of the perovskite-type oxide, a solid solution between $LaFeO_3$ and Pd is formed, where Pd is in distorted octahedral coordination and as a result of charge neutrality in higher oxidation state than 2+. The formal formula of this sample is $LaFe_{0.95}Pd_{0.05}O_{3\pm\delta}$. On the other hand, when $LaFeO_3$ is impregnated with the Pd salt, calcination generates supported PdO nano-particles and therefore, Pd in the oxidation state 2+. Actually, we have shown by XANES analysis that both Pd states populate $PdO/LaFeO_3$.[9] Thermal aging of $PdO/LaFeO_3$ causes variations of the ratio between the two observed Pd species.[15]

The observed Pd species demonstrate different effects on the catalytic activity of the two $LaFeO_3$-based materials.[9] It is immediately evident from Fig. 3(a) that $PdO/LaFeO_3$ is more active at lower temperature than $La(Fe,Pd)O_3$ for methane oxidation (O_2/CH_4 = 4) during a full heating-cooling cycle (200–900 °C). PdO exposed on $LaFeO_3$ is obviously the active phase. In contrast, the activity of $La(Fe,Pd)O_3$ is almost identical to that of $LaFeO_3$. Therefore, octahedral Pd cannot sustain catalytic activity in this temperature regime. Typically, the activity of a perovskite-type oxide above 500 °C is dictated by the oxygen supplied by the perovskite lattice (intrafacial mechanism).[16] Hence, Pd does not modify this property upon incorporation in the $LaFeO_3$ structure.

The cooling segment of the activity run of Fig. 3(a) is indicative of strong structural modifications upon attaining high temperature. The activity profile of $PdO/LaFeO_3$ exhibits a loss of *ca.* 25% between 700 and 550 °C that is typical of the formation of metallic Pd. At high temperature, PdO thermodynamically reduces to Pd^0 even under oxidizing conditions, a process that is well-known on conventional Pd-based methane oxidation catalysts.[17] Pd re-oxidation upon cooling regenerates the catalytic active PdO phase below 600 °C thus explaining the activity rise before extinction. Interestingly, the same activity profile is observed in the case of $La(Fe,Pd)O_3$. Assuming that the same reduction/re-oxidation process described for $PdO/LaFeO_3$ is valid, we conclude that during heating at temperatures above 700–800 °C octahedrally coordinated Pd segregates at the $LaFeO_3$ surface as Pd^0 thus causing the activity loss during cooling. At lower temperature Pd^0 re-oxidation causes a similar activity increase observed for $PdO/LaFeO_3$, but the gained activity is lower than for $PdO/LaFeO_3$ because of the partial re-incorporation of Pd into the $LaFeO_3$ structure. The process may be partial because restoration of the $LaFe_{0.95}Pd_{0.05}O_3$-like structure upon reduction and re-oxidation is temperature dependent: the lower the re-oxidation temperature the lower the fraction of octahedral Pd.[12]

Methane oxidation under lean conditions is a suitable probe reaction for the different Pd states. It allows structural information to be drawn during the reaction and it is a measure of the reactivity of different precious metal species. Fig. 3(a) reveals that if the activity profile of $PdO/LaFeO_3$ is compared to that of PdO/Al_2O_3, a tenfold higher surface area catalyst (Table 1), $PdO/LaFeO_3$ can be considered a good high temperature catalyst, but still inferior to PdO/ceria-zirconia, for example.[18] $LaFeO_3$ retards the spontaneous reduction of PdO: the temperature range in which the activity drop occurs is narrower and the activity loss is reduced compared to PdO/Al_2O_3. This function can be easily attributed to the strong interaction between palladium and $LaFeO_3$ that is reflected in the small fraction of octahedral Pd present in the sample. It can be speculated that PdO particles obtained after calcination are anchored to $LaFeO_3$ through the PdO_6-containing phase,[5] $LaFeO_3$ providing a reservoir for oxidized Pd in the high temperature regime where re-incorporation is still feasible.

Table 1. Physico-chemical properties of Pd-free and Pd-substituted $LaMnO_3$, $LaFeO_3$ and $LaCoO_3$.

sample	SSA [m²/g]	Pd content [wt%][a]	XRD[b]
$LaMnO_3$	20	–	pr
$La(Mn,Pd)O_3$	12	1.86	pr
$LaFeO_3$	14	–	po
$La(Fe,Pd)O_3$	14	1.95	po
$PdO/LaFeO_3$	13	1.98	po
$LaCoO_3$	6	–	pr
$La(Co,Pd)O_3$	9	1.90	pr
PdO/Al_2O_3	135	2	PdO, γ-Al_2O_3

[a]Determined by ICP-OES.[9,10] [b]p, perovskite; r, rhombohedral; o, orthorhombic.

Oscillating Reaction Conditions

$LaFeO_3$ is not very active for methane oxidation and improved catalytic activity was found only upon addition of palladium in the form of PdO particles. However, it has been shown above that we have been able to prepare a $LaFe_{0.95}Pd_{0.05}O_3$-like solid solution that is homogeneous with respect to the oxidation and coordination states of Pd. The apparent activation pathway shown in Fig. 3 indicates that it would be meaningful to exploit this property described for $LaFe_{0.95}Pd_{0.05}O_{3\pm\delta}$.[2] Therefore, $La(Fe,Pd)O_3$ was tested under redox oscillations (pulses of 60 s) at a representative temperature for automotive exhaust after-treatment of natural gas engines (500 °C). Redox oscillations are severe in these experiments, the target being the observation of structural changes associated with activity variations upon pulsing rather than working under realistic conditions of, for example, high frequency oscillations (~1 Hz) and complex exhaust composition.[19]

The *in situ* quick-EXAFS data collected for $La(Fe,Pd)O_3$ and PdO/Al_2O_3 demonstrate that at 500 °C palladium in the two catalysts periodically reduces and re-oxidizes according to the oxygen concentration modulation (Fig. 4(a)). However, the spectral changes are more important for $La(Fe,Pd)O_3$. In PdO/Al_2O_3, the spectrum obtained at the end of each O_2 pulse does not coincide with the fully oxidized state indicating that during the experiment the oxidation state of Pd reduces. This is confirmed by the data obtained after treatment using phase sensitive detection (PSD) to improve the S/N ratio and to enhance the subtle spectral changes induced by the repeated redox pulsing.[19,20] The phase-resolved spectra of both samples (Fig. 4(b)) show that the amplitude of the signal arising in correspondence with the Pd edge (24.350 keV) of $La(Fe,Pd)O_3$ is twice that of PdO/Al_2O_3. The amplitude of this signal is proportional to the oxidation state of the sample, its intensity coinciding with the energy shift indicated by arrows in Fig. 2. The larger the difference between initial and final oxidation state achieved during the experiment, the larger the amplitude change in the phase-resolved spectra. In the case of PdO/Al_2O_3, this amplitude change must correspond to the change from reduced Pd to partially oxidized Pd, the highest achievable oxidation state being 2+. However the time-resolved spectra indicate that re-oxidation is not complete. On the other hand, the intense edge energy signal for $La(Fe,Pd)O_3$ can be associated with the periodic reduction to Pd^0 and re-oxidation to an oxidation state that is larger than 2+ and that possibly corresponds to 3+ as indicated for $LaFe_{0.95}Pd_{0.05}O_{3\pm\delta}$.[2] This observation is considered the evidence that the protective function of the perovskite is at work under these conditions. Under oxidizing conditions, metallic Pd is re-oxidized and the strong interaction between the perovskite and the precious metal is restored. The absence of such interaction in the case of the alumina support prevents Pd from returning to the original oxidized state after every reduction pulse, thus causing the continuous reduction that at higher temperature induces particle sintering.

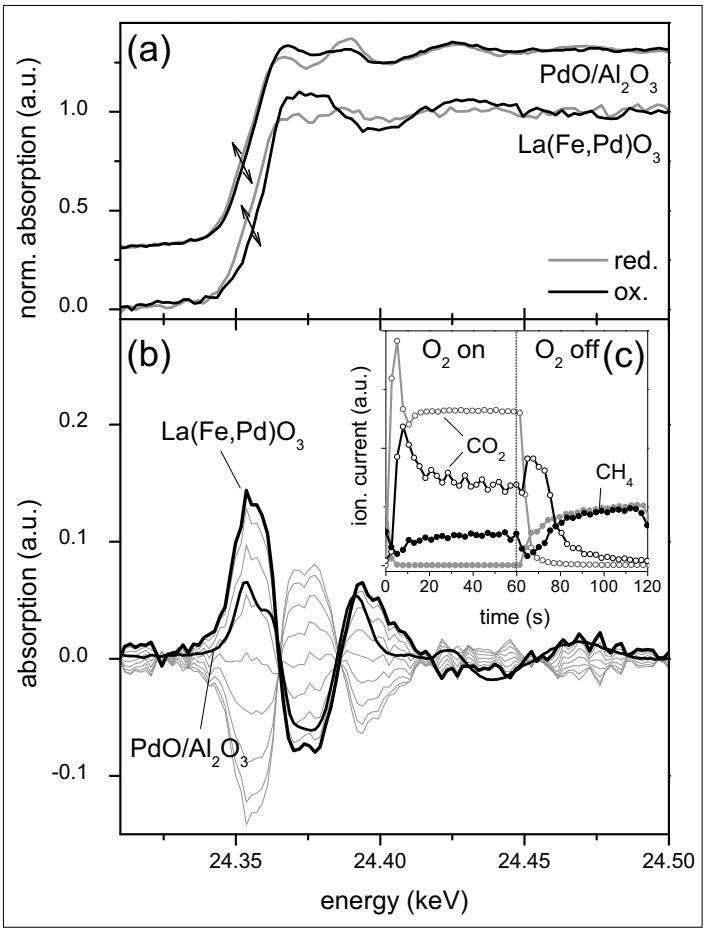

Fig. 4. (a) Selected time-resolved quick-EXAFS spectra of $La(Fe,Pd)O_3$ and PdO/Al_2O_3 representing oxidized and reduced states of Pd obtained during a modulation experiment consisting of 4 vol% O_2/He pulses in a 1 vol% CH_4/He flow at 500 °C (see ref. [19] for details). The arrows indicate the reversible shift of edge energy value in response to periodic reducing and oxidizing conditions. (b) Corresponding phase-resolved data; for PdO/Al_2O_3 only one spectrum is shown for simplicity. (c) MS data for m/z 44 (CO_2; ○ $La(Fe,Pd)O_3$, ○ PdO/Al_2O_3) and 15 (CH_4; ● $La(Fe,Pd)O_3$, ● PdO/Al_2O_3). Adapted from ref. [18].

The mass spectrometry (MS) data also demonstrate that such reversible periodic reduction/re-oxidation has positive effects on catalytic activity for methane oxidation. In correspondence with each pulse the concentration of methane is transiently reduced to a larger extent than at the end of each pulse, which represents steady state reaction conditions (Fig. 4(c)). This is confirmed by the corresponding transient increase of the CO_2 concentration at each pulse, which is not observed for PdO/Al_2O_3. Hence, the transient reduction and re-oxidation of Pd in $La(Fe,Pd)O_3$ evident from the QEXAFS data is associated with a transient enhancement of catalytic activity. The data obtained under periodic reaction conditions indicate the need to perform operando time-resolved measurements under representative reaction conditions in order to try to disclose the nature of the possible transient species responsible for this behaviour.

Typical Perovskite-type Oxidation Catalysts

In contrast to $LaFeO_3$, $LaMnO_3$ and $LaCoO_3$ are excellent oxidation catalysts.[1b] $LaMnO_3$ was shown to surpass Pt/Al_2O_3 for methane oxidation.[21] The addition of Pd to the perovskite structure can generate active materials with similar properties to those of $LaFe_{0.95}Pd_{0.05}O_3$. Pd- and Pt-substituted $LaCoO_3$ is promising for example for NO reduction by H_2[22] and for the water gas shift reaction,[23] respectively. Synthesis of $LaFeO_3$ and $LaMnO_3$ using ultrasonic spray combustion (USC) indicated that the oxidation and coordination states of Pd might be different from those proposed for $LaFe_{0.95}Pd_{0.05}O_{3\pm\delta}$.[24] Nishihata *et al.* reported the solubility regimes of Pd, Pt and Rh in a number of perovskite-type formulations.[25] They also demonstrated that the self-regenerative property observed for $LaFe_{0.95}Pd_{0.005}O_3$ was not valid for $LaMnO_3$ and $LaCoO_3$ because of the irreversible reduction of the perovskite lattice at high temperature.[26] Based on the acquired knowledge on the possible Pd species present on $La(Fe,Pd)O_3$ using XANES, $La(Mn,Pd)O_3$ and $La(Co,Pd)O_3$ were prepared by the amorphous citrate method and were characterized with respect to the oxidation and coordination state of Pd (Table 1).[10] The XANES spectra of fully oxidized $La(Mn,Pd)O_3$ and $La(Co,Pd)$

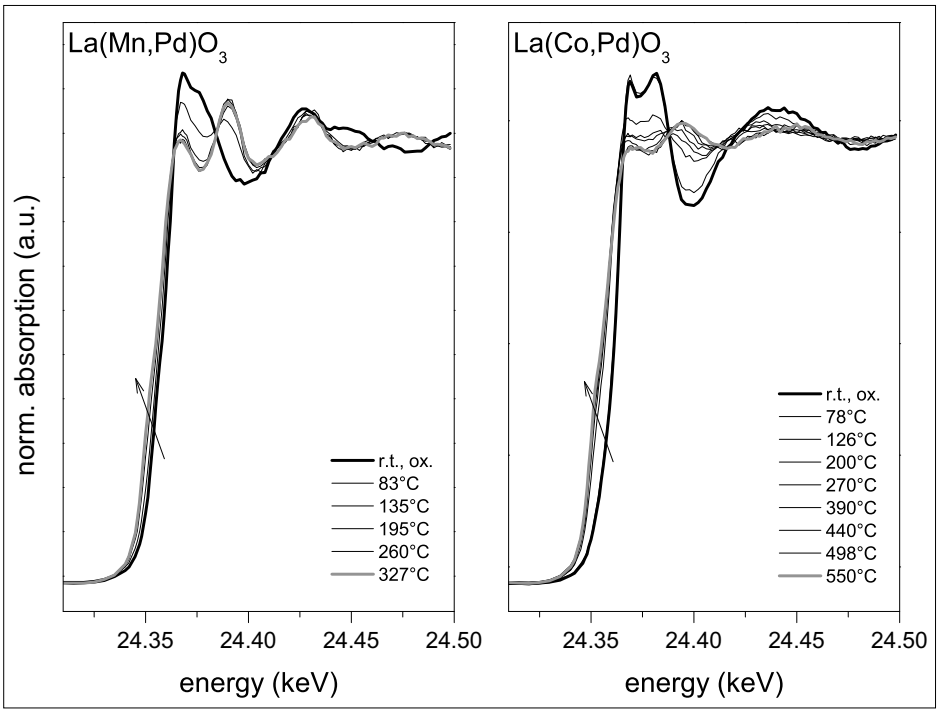

Fig. 5. Selected *in situ* fluorescence XANES spectra at the Pd K-edge during H_2-TPR of (a) $La(Mn,Pd)O_3$ and (b) $La(Co,Pd)O_3$ (5 vol% H_2/He). The arrows indicate the shift of energy upon reduction. Adapted from ref. [10].

O_3 samples display very similar features to those of $PdO/LaFeO_3$ and $La(Fe,Pd)O_3$, respectively (Fig. 1(b)). In particular $La(Co,Pd)O_3$ exhibits the same doublet of $La(Fe,Pd)O_3$ thus indicating the presence of distorted octahedrally coordinated Pd in oxidation state larger than 2+. On the contrary, $La(Mn,Pd)O_3$ was characterized by largely exposed PdO at the $LaMnO_3$ surface. The clear Pd-O-Pd second shell contribution appearing in the corresponding FT-EXAFS data (Fig. 1(c)) confirms the bulk character of the PdO particles. On the contrary, both $La(Fe,Pd)O_3$ and $La(Co,Pd)O_3$ present negligible contribution from shells other than the first, thus indicating the fine dispersion of Pd within $LaFeO_3$ and $LaCoO_3$.[27]

Despite the large structural difference, the reduction behaviour of $La(Mn,Pd)O_3$ and $La(Co,Pd)O_3$ followed by XANES is very similar (Fig. 5). Reduction of $La(Co,Pd)O_3$ occurs at lower temperature compared to $La(Fe,Pd)O_3$ which is in contradiction with the incorporation of Pd in $LaCoO_3$ evident from the XANES data. The contradiction is solved by comparison with the conventional H_2-TPR experiments demonstrating that PdO and $LaCoO_3$ reduce in the same temperature range. Because of the simultaneous and synergic reduction of $LaCoO_3$, Pd segregates from the perovskite structure at lower temperature.[27]

The different behavior of Pd when associated with Fe and Co or with Mn is attributed to the difference of ionic radius between the various cations and to the different chemistry and non-stoichiometry of perovskite-type oxides.[10] Possibly, also the crystal structure can play a role. The small Pd^{3+} cation can ideally fit in $LaFeO_3$ and $LaCoO_3$ structures, while Pd^{2+} is more appropriate for $LaMnO_3$ thus providing Pd segregation during synthesis. This copes with the generally higher average oxidation state of Mn in the perovskite structure compared with that of Co or Fe.[1a]

Obviously, the manganate and cobaltate samples exhibited significantly different catalytic activity for methane oxidation under lean conditions as a consequence of the different oxidation and coordination states of Pd (Fig. 3(b)). Exposure of the PdO phase on $LaMnO_3$ produced the best low-temperature activity. $La(Co,Pd)O_3$ displayed very similar activity to $La(Fe,Pd)O_3$ thus confirming the inactivity of Pd buried in the perovskite lattice for this reaction.

Conclusions

Dispersed palladium on perovskite-type mixed oxides is a potential catalyst for three-way catalysis, where the oxidation activity of the support is completed by the reduction and the oxidation activity of the precious metal. Our work shows that the structure of the precious metal-based catalysts needs to be carefully ascertained. The solid solution between the perovskite-type oxide and the precious metal is advantageous for methane oxidation under lean conditions only if the material is exposed to temperatures above 700 °C. Generally, oxidation activity is determined by the mixed metal oxide, but interactions between the perovskite support and palladium reduce the temperature range in which PdO is thermodynamically instable thus retarding PdO decomposition and aging phenomena. The strong interaction between the precious metal and the perovskite-type oxide can be fruitfully exploited to grant enhanced redox activity that is characteristic of three-way catalysts. We have shown that such a possibility is strongly dependent on perovskite composition and is not equally valid for the three classes of materials discussed here. The origin of this difference lies in the reducibility of the perovskite, which is dependent on the nature of the selected metal cations, including Pd.

Finally, it should be emphasized that the intimate interaction between a perovskite matrix and Pd is not a characteristic of Pd only but can be associated with transition and coinage metals in a broader view. Therefore, the 'self-regenerative' property can be used in a wider application range where other elements than precious metals are used.[1a] It certainly represents a fascinating strategy to prepare catalysts with new and unusual properties.

Acknowledgments

The authors are grateful to Empa and SNF-NRP62 'Smart Materials' for financial support. The European Synchrotron Radiation Facility (ESRF), the Swiss Light Source (SLS) and Hasylab at DESY are acknowledged for their continued support through beam time allocation and Dr. O. Safonova for the simulation of the XANES spectra.

Received: July 9, 2012

[1] a) M. A. Pena, J. L. G. Fierro, *Chem. Rev.* **2001**, *101*, 1981; b) S. Royer, D. Duprez, *ChemCatChem* **2011**, *3*, 24.
[2] Y. Nishihata, J. Mizuki, T. Akao, H. Tanaka, M. Uenishi, M. Kimura, T. Okamoto, N. Hamada, *Nature* **2002**, *418*, 164.
[3] a) G. Qi, W. Li, *Catal. Today* **2012**, *184*, 72; b) C. H. Kim, G. Qi, K. Dahlberg, W. Li, *Science* **2010**, *327*, 1624.
[4] R. J. H. Voorhoeve, D. W. Johnson, J. P. Remeika, P. K. Gallagher, *Science* **1977**, *195*, 827.
[5] J. P. Dacquin, M. Cabié, C. R. Henry, C. Lancelot, C. Dujardin, S. R. Raouf, P. Granger, *J. Catal.* **2010**, *270*, 299.
[6] 'Climate Change 2007: The Physical Science Basis, Contribution of Working Group I to the Fourth Assessment Report of IPCC', Eds. S. Solomon, D. Qin, M. Manning, Z. Chen, M. Marquis, K. B. Averyt, M. Tignor, in Cambridge University press, Cambridge, **2007**, p. 212.
[7] I. Rossetti, L. Forni, in 'Synthesis, properties, and applications of oxide nanomaterials', Eds. J. A. Rodriguez, M. Fernandez-Garcia, John Wiley & Sons, Inc., Hoboken, New Jersey, **2007**, p. 563.
[8] a) E. Tzimpilis, N. Moschoudis, M. Stoukides, P. Bekiaroglou, *Appl. Catal. B: Environ.* **2008**, *84*, 607; b) D. Fino, N. Russo, G. Saracco, V. Specchia, *Progr. Solid State Chem.* **2007**, *35*, 501.

[9] A. Eyssler, P. Mandaliev, A. Winkler, P. Hug, O. Safonova, E. Figi, A. Weidenkaff, D. Ferri, *J. Phys. Chem. C* **2010**, *114*, 4584.
[10] A. Eyssler, A. Winkler, O. Safonova, M. Nachtegaal, M. Santhosh Kumar, P. Hug, A. Weidenkaff, D. Ferri, *Chem. Mater.* **2012**, *24*, 1864.
[11] M. S. G. Baythoun, F. R. Sale, *J. Mater. Sci.* **1982**, *17*, 2757.
[12] S. J. Kim, S. Lemaux, G. Demezeau, J. Y. Kim, J. H. Choy, *Mater. Chem.* **2002**, *12*, 995.
[13] M. Uenishi, M. Taniguchi, H. Tanaka, M. Kimura, Y. Nishihata, J. Mizuki, T. Kobayashi, *Appl. Catal. B* **2005**, *57*, 267.
[14] J. A. van Bokhoven, H. Sambe, D. E. Ramaker, D. C. Koningsberger, *J. Phys. Chem. B* **1999**, *103*, 7557.
[15] A. Eyssler, A. Winkler, P. Mandaliev, P. Hug, A. Weidenkaff, D. Ferri, *Appl. Catal. B* **2011**, *106*, 494.
[16] J. L. G. Fierro, *Catal. Today* **1990**, *8*, 153.
[17] a) M. Santhosh Kumar, M. H. Aguirre, A. Weidenkaff, D. Ferri, *J. Phys. Chem. C* **2010**, *114*, 9439; b) R. Farrauto, M. Hobson, T. Kennelly, E. Waterman, *Appl. Catal. A* **1992**, *81*, 227.
[18] M. Santhosh Kumar, A. Eyssler, P. Hug, N. vanVegten, A. Baiker, A. Weidenkaff, D. Ferri, *Appl. Catal. B* **2010**, *94*, 77.
[19] A. Eyssler, E. Kleymenov, A. Kupferschmid, M. Nachtegaal, M. Santhosh Kumar, P. Hug, A. Weidenkaff, D. Ferri, *J. Phys. Chem. C* **2011**, *115*, 1231.
[20] D. Ferri, M. Santosh Kumar, R. Wirz, A. Eyssler, O. Korsak, P. Hug, A. Weidenkaff, M. A. Newton, *PCCP* **2010**, *12*, 5634.
[21] H. Arai, T. Yamada, K. Eguchi, T. Seiyama, *Appl. Catal.* **1986**, *26*, 265.
[22] G. L. Chiarello, D. Ferri, J. D. Grunwaldt, L. Forni, A. Baiker, *J. Catal.* **2007**, *252*, 137.
[23] R. Watanabe, Y. Sekine, H. Takamatsu, Y. Sakamoto, S. Aramaki, M. Matsukata, E. Kikuchi, *Top. Catal*. **2010**, *53*, 621.
[24] X. Wei, P. Hug, R. Figi, M. Trottmann, A. Weidenkaff, D. Ferri, *Appl. Catal. B* **2010**, *94*, 27.
[25] H. Tanaka, M. Taniguchi, M. Uenishi, N. Kajita, I. Tan, Y. Nishihata, J. Mizuki, K. Narita, M. Kimura, K. Kaneko, *Angew. Chemie Int. Ed.* **2006**, *45*, 5998.
[26] I. Tan, H. Tanaka, M. Uenishi, K. Kaneko, S. Mitachi, *J. Ceram. Soc. Jpn.* **2005**, *113*, 71.
[27] G. L. Chiarello, J. D. Grunwaldt, D. Ferri, F. Krumeich, C. Oliva, L. Forni, A. Baiker, *J. Catal.* **2007**, *252*, 127.